Unique Pathology in Simian Immunodeficiency Virus-Infected Rapid Progressor Macaques Is Consistent with a Pathogenesis Distinct from That of Classical AIDS$^\nabla$

Charles R. Brown,[1] Meggan Czapiga,[2] Juraj Kabat,[2] Que Dang,[1] Ilnour Ourmanov,[1] Yoshiaki Nishimura,[1] Malcolm A. Martin,[1] and Vanessa M. Hirsch[1]*

Laboratory of Molecular Microbiology[1] and Research Technology Branch,[2] NIAID, NIH, 4 Center Drive, Bethesda, Maryland 20892

Simian immunodeficiency virus (SIV) infection of macaques and human immunodeficiency virus type 1 (HIV-1) infection of humans result in variable but generally fatal disease outcomes. Most SIV-infected macaques progress to AIDS over a period of 1 to 3 years, in the face of robust SIV-specific immune responses (conventional progressors [CP]). A small number of SIV-inoculated macaques mount transient immune responses and progress rapidly to AIDS (rapid progressors [RP]). We speculated that the underlying pathogenic mechanisms may differ between RP and CP macaques. We compared the pathological lesions, virus loads, and distribution of virus and target cells in SIVsmE660- or SIVsmE543-infected RP and CP rhesus macaques at terminal disease. RP macaques developed a wasting syndrome characterized by severe SIV enteropathy in the absence of opportunistic infections. In contrast, opportunistic infections were commonly observed in CP macaques. RP and CP macaques showed distinct patterns of CD4$^+$ T-cell depletion, with a selective loss of memory cells in RP macaques and a generalized (naive and memory) CD4 depletion in CP macaques. In situ hybridization demonstrated higher levels of virus expression in lymphoid tissues ($P < 0.001$) of RP macaques and a broader distribution to include many nonlymphoid tissues. Finally, SIV was preferentially expressed in macrophages in RP macaques whereas the primary target cells in CP macaques were T lymphocytes at end stage disease. These data suggest distinct pathogenic mechanisms leading to the deaths of these two groups of animals, with CP macaques being more representative of HIV-induced AIDS in humans.

Human immunodeficiency virus type 1 (HIV-1), the causative agent of AIDS in humans, results in a progressive depletion of CD4$^+$ T lymphocytes that culminates in fatal immunodeficiency. Although it is clear that HIV is responsible for massive early destruction of memory CD4$^+$ T lymphocytes (7), the subsequent disease course is prolonged and variable, suggesting additional mechanisms in the chronic stages of the disease. The long asymptomatic period of infection is associated with increased immune activation particularly of the remaining memory CD4$^+$ T cells, increased rates of spontaneous apoptosis, abnormalities in CD4$^+$ T-cell function (13, 14, 20, 21, 24), and destruction of the lymphoid architecture (69). The degree of T-cell activation has value in predicting HIV infection survival time (13, 24). This has led many to suggest that the mechanisms underlying AIDS are more complex than a simple model of slow virus-induced CD4$^+$ T-cell death (6, 18, 28, 29).

Simian immunodeficiency virus (SIV) originating in sooty mangabey monkeys is perhaps the most relevant model of human AIDS currently available. This lineage includes the virus most commonly used in the field, SIVmac239, which arose following the introduction of SIVsm into rhesus macaques housed in U.S. primate centers (12, 71). However, equally relevant models have been developed by using SIVsm

strains from captive sooty mangabeys, including the closely related SIVsmE660 and molecularly cloned SIVsmE543-3 strains derived in our laboratory (1, 31, 34, 35, 42, 63). SIVsm/mac and HIV are remarkably similar in terms of biology and pathogenesis in vivo. Both target CD4$^+$ cells, including T cells and macrophages, and use the chemokine coreceptor CCR5, resulting in direct destruction of memory CD4$^+$ T cells at mucosal sites (7, 48, 50, 60, 66). SIV infection of macaques covers a continuum in terms of rate of disease progression, similar to HIV infection of humans (5, 19, 31, 33, 34, 38, 49, 62, 73, 79). The level at which the virus stabilizes following primary infection is predictive of the rate of disease progression in both SIV and HIV infections (33, 53, 76). Both are associated with intense immune activation during the chronic phase of disease (13, 24, 48, 70, 72), and the pathological manifestations of AIDS are similar (5, 47, 51, 71). End stage disease is characterized by terminal blood and tissue CD4$^+$ T-cell depletion, infections with a variety of opportunistic pathogens (5, 47, 51, 71), and the development of virus-induced encephalitis (3, 17, 26, 57, 61, 62, 68, 81, 82).

Despite remarkable similarities between simian AIDS and human AIDS, there are a number of differences that must be considered. First, the disease course of SIV infection of macaques is compressed relative to that of HIV infection, with a median survival time of 1 to 3 years versus 10 years in untreated human AIDS. Second, SIVsm/mac virus isolates use CCR5 as their primary coreceptor; the emergence of CXCR4-using isolates observed in many human AIDS patients is only rarely observed in SIV infection (45). However, since isolates

* Corresponding author. Mailing address: LMM, NIAID, NIH, Building 4, Room B1-41, 4 Center Drive, Bethesda, MD 20892. Phone: (301) 496-0559. Fax: (301) 480-3129. E-mail: vhirsch@niaid.nih.gov.

TABLE 1. Summary of clinical and pathological outcomes of study animals

Category and macaque	Virus	Survival time (wk)	Major pathological findings
RP			
H147	E660	14	SIVE and pneumonia with MNGC, severe enteritis (protozoal), MNGC in GI tract and prostate
H168	E660	22	SIVE and pneumonia with MNGC, severe enteritis, MNGC in lymph nodes
H538	E660	9	SIVE and pneumonia with MNGC, severe enteritis, MNGC in ovary and fallopian tube
H567	E660	10	SIVE and mild pneumonia with MNGC, severe enteritis, MNGC in lymph nodes and GI tract
H426	E660	20	SIVE and pneumonia with MNGC, severe enteritis, MNGC in GI tract and eye
18655	E660	16	SIVE and pneumonia with MNGC, severe enterocolitis, MNGC in thymus, lymph nodes, spleen, GI tract, kidney, and testis
H445	E543-3	15	SIVE and pneumonia with MNGC, severe enteritis
CK2F	E543-3	31	Mild diffuse SIVE, pneumonia with MNGC, severe enteritis
CK2K	E543-3	15	SIVE and pneumonia, severe lymphoid depletion with MNGC, moderate-to-severe enteritis
CP			
H119	E660	51	Disseminated *M. avium* enteritis and lymphadenitis, lymphoid hyperplasia and involution lymphoma (mesenteric lymph node), focal SIVE
H120	E660	54	*M. avium* enteritis, lymphadenitis, lymphoid hyperplasia and involution
H133	E660	58	*P. carinii* pneumonia, enteritis, lymphoid depletion
H187	E660	54	Pyogranulomatous lymphadenitis, cytomegalovirus orchitis, lymphoid depletion
H454	E660	72	Multicentric lymphoma (heart, adrenals, urinary bladder, ovaries, eye)
H063	E543-3	164	*M. avium* enteritis and lymphadenitis, lymphoid depletion
H460	E543-3	100	Cryptosporidial enteritis, cholecystitis, cholangiohepatitis, lymphoid depletion
XGE	E543-3	77	Suppurative pneumonia with pulmonary thrombosis, lymphoid depletion, enteritis with amyloidosis
H679	E543-3	60	Abscessation of kidney, secondary peritonitis (*Staphylococcus aureus*), lymphoid depletion

recovered early in infection with HIV preferentially use CCR5 as a coreceptor, the pathogenesis of SIV and that of HIV appear more similar to one another than to that of CXCR4-using SIV-HIV isolates (39, 60). Third, while rare individuals infected with HIV-1 rapidly develop disease (22, 23, 54, 80), the frequency of an accelerated disease course is much higher in SIV-infected macaques. About 10 to 25% of rhesus macaques inoculated with pathogenic strains of SIVmac/sm fail to mount measurable immune responses and develop disease in less than 6 months (5, 16, 34, 71, 79). Finally, the pathology of simian AIDS includes descriptions of SIV-induced disease in which multinucleated giant cells (MNGC) in the lymphoid tissues, brain, and lungs are a prominent feature (5, 47, 51). With the exception of the brains of HIV-infected patients with encephalitis, MNGC are rarely observed in tissues of humans with AIDS. In our studies, the presence of MNGC was associated with extremely high viremia and transient immune responses, both signs of rapid progression (31, 37, 46). Retrospective studies have also shown that SIV encephalitis (SIVE) is highly correlated with rapid disease progression (3, 61, 62, 77). We speculated that rapid progression of SIV infection of macaques might constitute a unique pathological syndrome, distinct from the classical descriptions of SIV-induced AIDS. The goal of the present study was to compare pathology, virus distribution, and target cells by in situ hybridization (ISH) and confocal microscopy in terminal tissues of conventional progressors (CP) and rapid progressors (RP) infected with SIVsmE660 or SIVsmE543-3.

MATERIALS AND METHODS

Viruses and animal study design. The rhesus macaques evaluated in this study were inoculated intravenously with either uncloned SIVsmE660 (33, 34, 37) or the molecular clone SIVsmE543-3 (31, 33). These isolates are closely related genetically (92% identity in envelope) to one another and were derived by macaque passage from the SIVsmF236 isolate from the Tulane National Primate Research Center. SIVsmF236 was derived by one macaque passage of virus from a naturally infected sooty mangabey monkey (5).

Study animals were selected from a group of 72 SIVsm-infected Indian rhesus macaques (25, 49). This group of animals included nine RP (see Table 1) that were identified by a lack of SIV-specific antibody responses by 4 weeks postinoculation and progression to disease in 6 months or less. CP macaques for comparison were chosen on the basis of seroconversion and survival for 1 year or longer; any animals that died prematurely because of unrelated causes, such as anesthetic accidents, were eliminated. The CP macaques selected for the present study were not significantly different from the remainder of the CP macaques in the cohort in terms of CD4+ T-cell numbers at the time of euthanasia (mean CD4 count of 85 versus 188/μl; $P = 0.11$) or survival time (median survival time of 58 versus 76 weeks; $P = 0.27$).

The same clinical criteria were used for euthanasia in both groups. All animals were euthanized if they lost >20% of their body weight or developed intractable diarrhea that was unresponsive to supportive or antibiotic treatment, respiratory signs with radiographic evidence of pneumonia, persistent anorexia and lethargy, or neurologic signs. Animals were exsanguinated under deep anesthesia, perfused with 1 liter of saline, followed by 1 liter of 10% buffered formalin, prior to collection of tissues. Representative samples were taken for formalin fixation. All sections were stained with hematoxylin and eosin for routine histopathology. All animals were housed in accordance with American Association for Accreditation of Laboratory Animal Care standards. The investigators adhered to the Guide for the Care and Use of Laboratory Animals prepared by the Committee on Care and Use of Laboratory Animals of the Institute of Laboratory Resources, National Resource Council, and the NIAID Animal Care and Use Committee-approved protocols.

Lymphocyte immunophenotyping. EDTA-anticoagulated blood samples were collected sequentially for analysis of plasma viral RNA loads and lymphocyte subsets by flow cytometry. EDTA-treated blood samples were stained for flow cytometric analysis as described previously (58, 60), by using combinations of the following fluorochrome-conjugated monoclonal antibodies: CD3 (fluorescein isothiocyanate [FITC] or phycoerythrin [PE]), CD4 (PE, peridinin chlorophyll protein-Cy5.5 [PerCP-Cy5.5], or allophycocyanin [APC]), CD8 (PerCP or APC), CD28 (FITC or PE), CD95 (APC), and Ki-67 (FITC or PE). All antibodies were obtained from BD Biosciences (San Diego, CA), and samples were analyzed by four-color flow cytometry (FACScalibur; BD Biosciences Immunocytometry Systems). Analysis of data was performed with CellQuest Pro (BD Biosciences) and FlowJo (TreeStar, Inc., San Carlos, CA). In this study, naive CD4+ T cells were identified by their CD95low CD28high phenotype, whereas memory CD4+ T cells were CD95high CD28high or CD95high CD28low in the CD4+ small lymphocyte gate (60, 67).

Plasma SIV RNA quantitation. A plasma SIV RNA viral load real-time quantification assay based on the Applied Biosystems Prism Sequence Detection
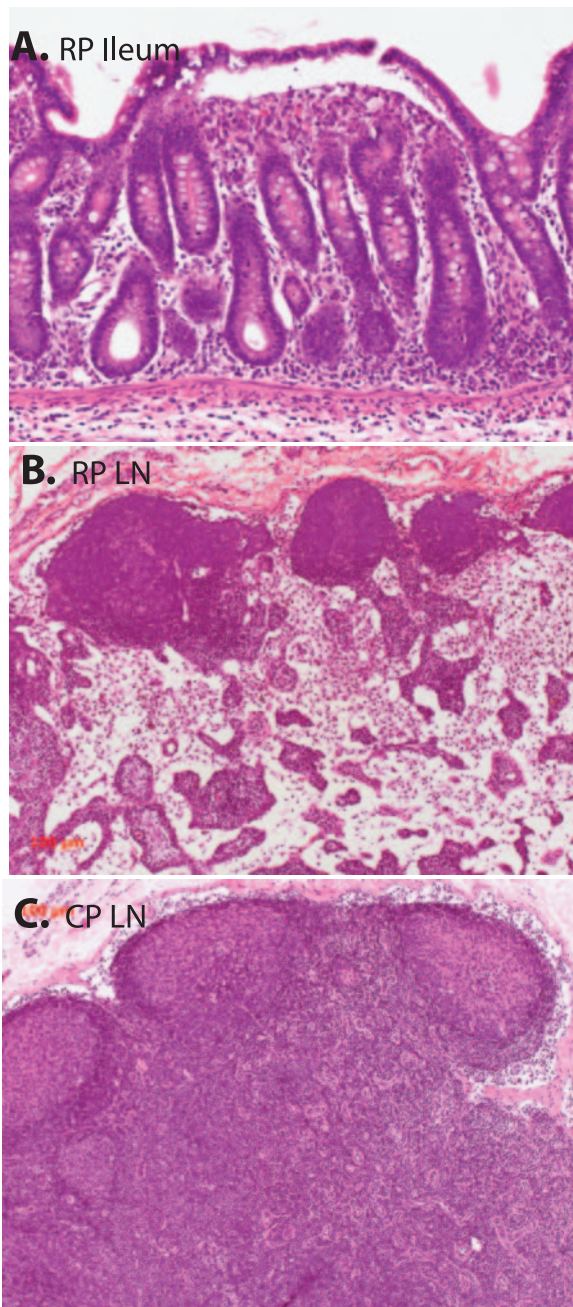
FIG. 1. Hematoxylin-and-eosin-stained sections of the ileum of an RP (top) and comparison of the lymph nodes (LN) of a representative RP macaque and a CP macaque. (A) Section of ileum of RP macaque H445 showing the blunting and fusion of intestinal villi that was characteristic of RP intestinal tissues. (B) Mesenteric lymph node of RP macaque H445 showing depletion of the paracortex and a lack of secondary germinal centers. (C) Inguinal lymph node of CP macaque H133 showing large germinal centers with irregular mantles and hyalinization indicative of involution.

System was used as previously described (74). Viral RNA was isolated from plasma with a QIAamp viral RNA kit (QIAGEN Inc., Santa Clarita, CA) and treated with amplification grade DNase I (Life Technologies, Gaithersburg, MD) as recommended by the manufacturer. Replicate aliquots of the test RNA were subjected to RT-PCR by a two-step, two-enzyme protocol with SIV-Gag consensus primers S-GAG03 and S-GAG04 and SIV-Gag consensus TaqMan probe
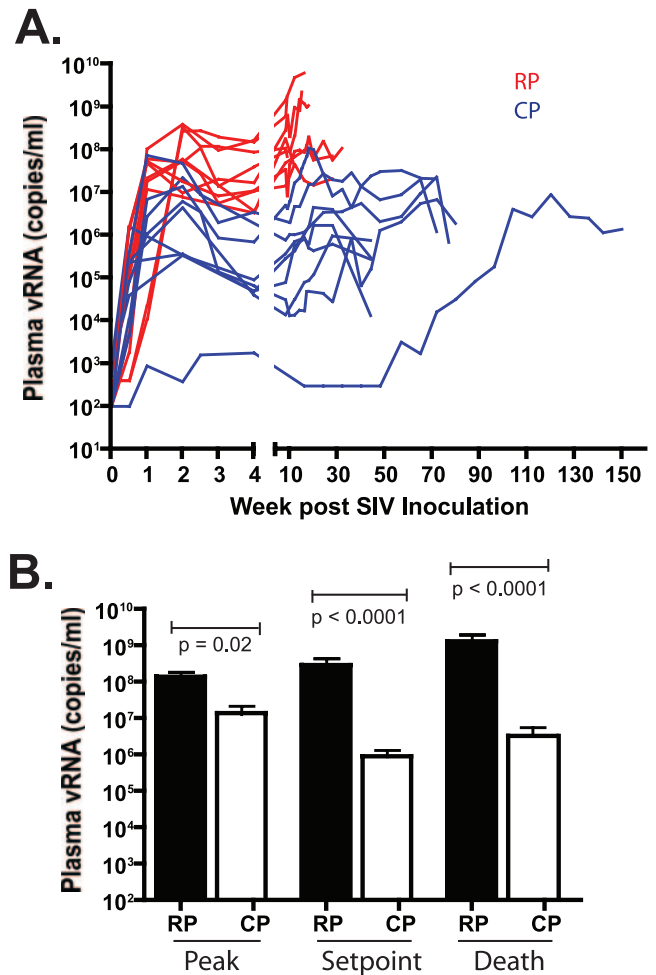
FIG. 2. Plasma viremia in RP and CP macaques is shown over the time course of infection. (A) Sequential plasma viral loads in RP (red) and CP (blue) macaques. (B) Comparison of peak, set point, and terminal plasma viral RNA levels in RP and CP macaques with statistically significant differences between the two groups at each of these time points (Mann-Whitney U test).

P-SUS-05. The poly(A)-tailed full-length RNA control template was purified on oligo(T)-agarose and quantified by A_{260} measurements based on the calculated extinction coefficient for the transcript sequence. A serial fivefold dilution series of the standard RNA template was assayed in duplicate to generate a standard curve for each assay. RT-PCR for each plasma sample was performed in triplicate. Assay results were normalized to the volume of plasma extracted and expressed as numbers of SIV RNA copy equivalents per milliliter of plasma, as described for HIV-1 (64, 65). Interassay variation was less than 25% (confidence value).

SIV-specific ISH. Formalin-fixed, paraffin-embedded tissues were assayed for SIV viral RNA expression by ISH as previously described (32). Briefly, the sections were hybridized overnight at 50°C with either a sense or an antisense SIVmac239 digoxigenin-UTP-labeled riboprobe. The hybridized sections were blocked with 3% normal sheep and horse serum in 0.1 M Tris, pH 7.4, and then incubated with sheep anti-digoxigenin–alkaline phosphatase (Roche Molecular Biochemicals) and nitroblue tetrazolium–5-bromo-4-chloro-3-indolyl-β-D-galactopyranoside (BCIP; Vector Labs). ISH-stained tissues from mesenteric lymph nodes and the gastrointestinal (GI) tract (gut-associated lymphoid tissue [GALT] and lamina propria) were visualized and photographed with a Zeiss Axiophot microscope. Five representative fields of view of each stained tissue section were photographed and analyzed. The number of SIV+ cells was calculated by using a segmentation function in the IPLab software (Scanlytics Inc., Rockville, MD). SIV+ cells in several ISH-stained control sections were counted
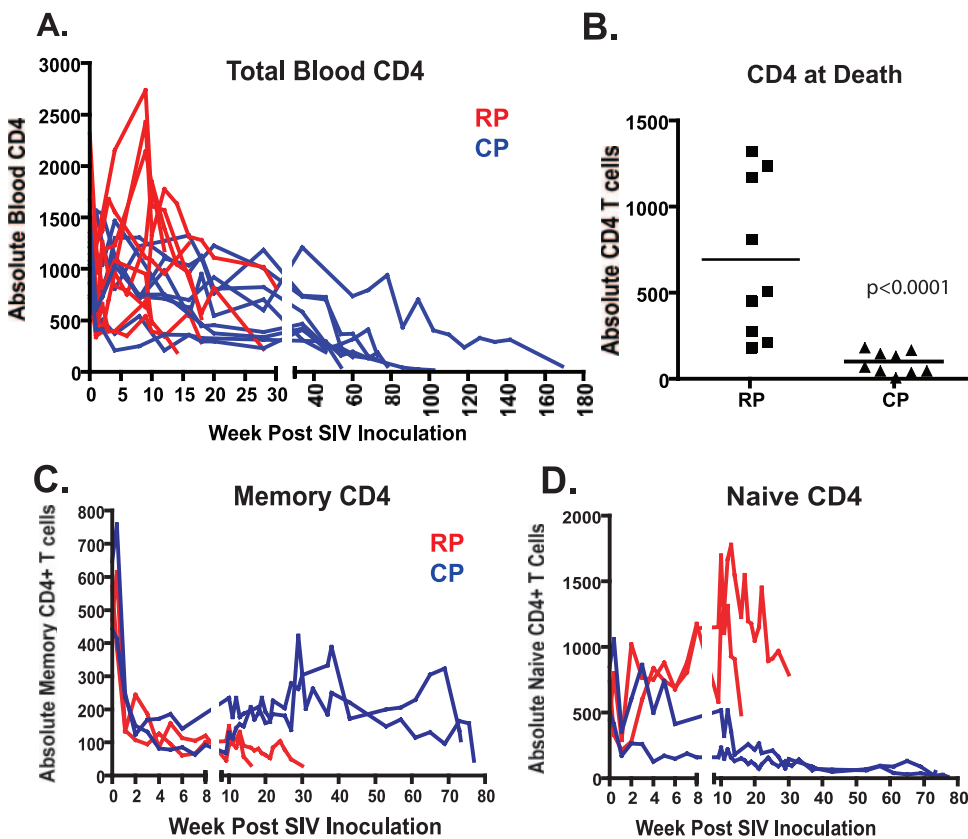
FIG. 3. CD4$^+$ T cells in the peripheral blood of RP and CP macaques over the time course of infection. (A) Total CD4$^+$ T cells are compared in RP (red) and CP (blue) macaques. (B) Comparison of total CD4$^+$ T cells in peripheral blood at the time of euthanasia shows significantly lower total CD4$^+$ T-cell counts in CP versus RP macaques (Mann-Whitney U test). Comparison of memory (C) and naive (D) CD4$^+$ T cells in the blood of two RP and two CP macaques inoculated with SIVsmE543-3 shows the selective depletion of memory CD4$^+$ T cells that occurs in RP macaques, as determined by CD28 and CD95 expression. In contrast, CP macaques demonstrate early depletion of memory CD4$^+$ T cells with partial replenishment but subsequent progressive loss of both memory and naive CD4$^+$ T-cell subsets during long-term progression.

manually, and the size and threshold values for the automatic segmentation function were determined.

Confocal microscopy to identify SIV-expressing cells. Formalin-fixed, paraffin-embedded tissues were stained for SIV viral RNA by ISH by a modified method previously described (31). Briefly, the sections were stained with the same SIV probe and procedure as mentioned above, with the following changes. The samples were treated with methanol-hydrogen peroxide, and the hybridized tissue sections were incubated with sheep anti-digoxigenin–horseradish peroxidase (SAD-HRP; Roche Molecular Biochemicals). SAD-HRP was detected by a fluorescent tyramide signal amplification technique (TSA Plus FITC, NEL741; Perkin-Elmer). After completion of the ISH assay, the sections were incubated in mouse anti-human macrophage antibody (HAM56; DAKO M0632) and stained with goat anti-mouse immunoglobulin M-Alexa 633 (Invitrogen) and then incubated with rabbit anti-human CD3 (T-cell marker; DAKO A0452), followed by goat Alexa 594 anti-rabbit immunoglobulin G antibody. The triple-stained sections were mounted in Vectashield Hardset mounting medium (Vector Laboratories, Burlingame, CA) and photographed with a Leica confocal scanning microscope. Ten representative 40× fields of mesenteric lymph node and ileum tissues from five RP macaques and four CP macaques were photographed, and the SIV$^+$ T cells and macrophages were counted.

Statistical analyses. Viral loads in plasma, numbers of CD4$^+$ T cells in blood, and numbers of SIV-expressing cells in tissues were compared by unpaired two-tailed *t* tests with GraphPad Prism (San Diego, CA), and Kaplan-Meier survival plots were compared by using log rank tests.

RESULTS

A retrospective analysis was undertaken to examine end stage virus distribution and infected target cells in rhesus macaques inoculated with SIVsm (25, 33, 49) that progressed rapidly (RP macaques) or underwent conventional progression (CP macaques) to disease. As shown in Table 1, RP macaques developed an illness that necessitated euthanasia significantly earlier than CP macaques, with a median survival of 15 versus 72 weeks (log rank test; *P* = 0.001).

The apparent disease phenotypes in RP and CP macaques also appeared to be quite distinct. RP macaques succumbed to a wasting syndrome with chronic diarrhea. Pathological findings in these macaques included severe enteritis, characterized by villus blunting, and fusion, as shown in a representative section of ileum in Fig. 1A, similar to the SIV enteropathy previously described in SIV infection (30, 75, 78) and are in keeping with the major impact of SIV on the GI tract (75). Opportunistic infections (OIs) were not observed in either the GI tract or other organs, suggesting that clinical disease in these animals was the direct result of SIV infection rather than secondary to immune suppression. In addition to enteritis, SIV-induced pneumonia and SIVE with MNGC were consistently observed in RP macaques and MNGC were frequently observed in a variety of other tissues (Table 2). RP macaques did not develop reactive lymphoid hyperplasia as assessed by sequential peripheral lymph node measurements (data not shown), and consistent with this observa-

Rapid Progressor   **Conventional Progressor**
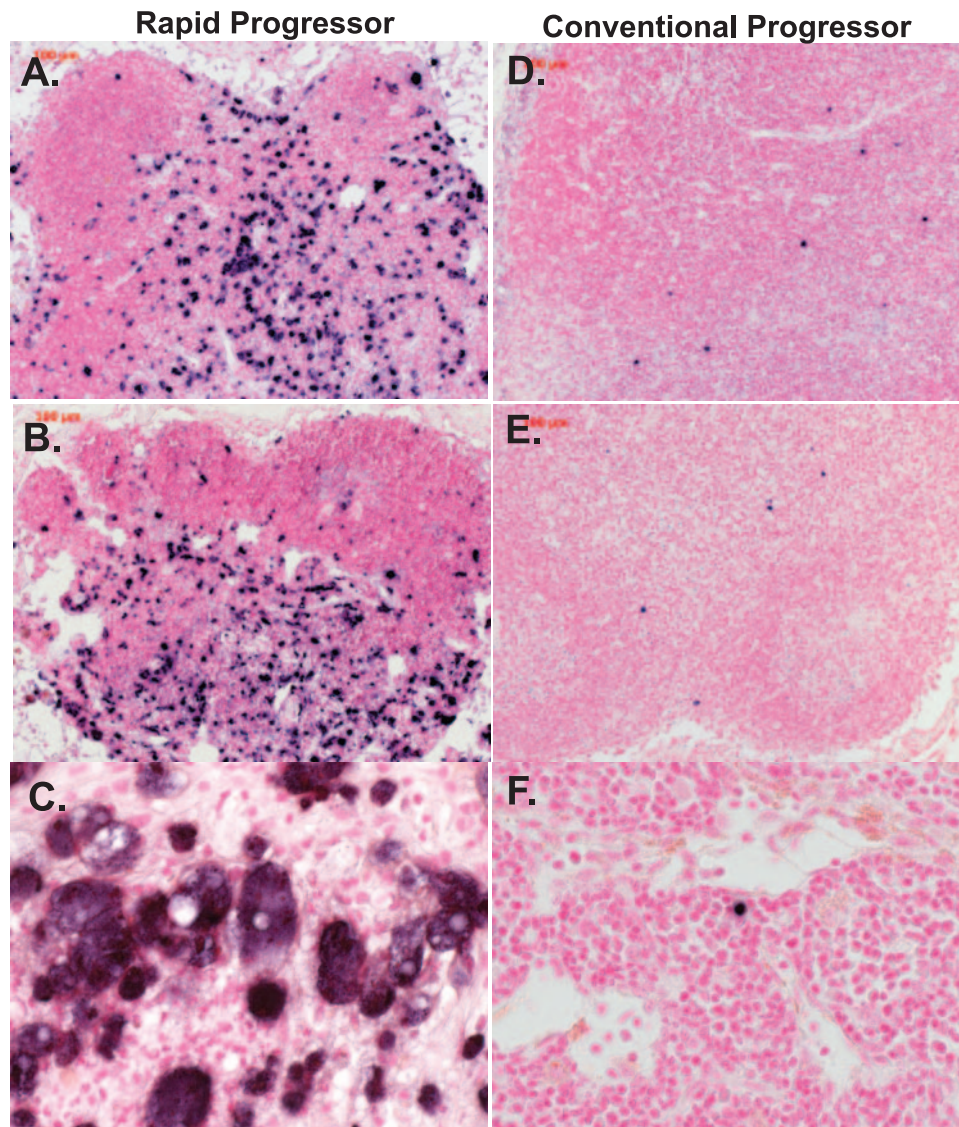
FIG. 4. Representative fields of view of ISH for SIV viral RNA in the mesenteric lymph nodes of RP and CP macaques. (A, B, and C) RP lymph nodes showing numerous SIV-expressing cells (dark blue) within the paracortex, follicle, intrafollicular zone, and cortex of the lymph nodes of SIV-infected RP macaques H538 (A; magnification, ×10), H445 (B; magnification, ×10), and H168 (C; magnification, ×40) showing large numbers of SIV-expressing cells. Lower numbers of SIV-expressing cells were observed in the mesenteric lymph nodes of representative CP macaques H063 (D), H119 (E), and H460 (F). Magnification, ×40.

tion, lymph nodes were relatively quiescent, with a lack of germinal centers (Fig. 1B).

In contrast, CP macaques presented with a disease syndrome more similar to human AIDS. As shown in Table 1, OIs with agents such as *Mycobacterium avium* (n = 3), *Pneumocystis carinii* (n = 1), cryptosporidia (n = 1), cytomegalovirus (n = 1), or overwhelming bacterial infections were commonly seen in CP macaques (n = 2). Lymphoma, presumably due to Epstein-Barr virus infection, was also observed (n = 1). SIVE was only rarely observed in CP macaques (H119) and was considerably less severe than in RP macaques. MNGC were only rarely observed in tissues of CP macaques (H460, H119). CP macaques had evidence of prior reactive lymphoid hyperplasia with prominent germinal centers often in the process of involution and fibrosis (Fig. 1C).

Prior to the evaluation of end stage tissues, sequential plasma viral loads and circulating $CD4^+$ T-cell levels of the two groups were compared. As shown in Fig. 2, RP macaques exhibited higher levels of plasma viral RNA at peak ($P = 0.02$), set point ($P < 0.0001$), and death ($P < 0.0001$) than CP macaques. By the time of euthanasia, plasma viral RNA levels of RP macaques were 2 to 3 logs higher than those of CP macaques. The two SIV-infected cohorts also differed with respect to circulating $CD4^+$ lymphocyte counts at the time of euthanasia. As shown in Fig. 3A, only modest $CD4^+$ T-cell depletions were observed in either group during the first 30 weeks of infection (37 versus 16% decline in RP and CP, respectively). At 30 weeks, the extent of depletion did not differ significantly between the two groups (Mann-Whitney U test, $P > 0.05$). Many of the RP macaques were euthanized

Rapid Progressor   Conventional Progressor
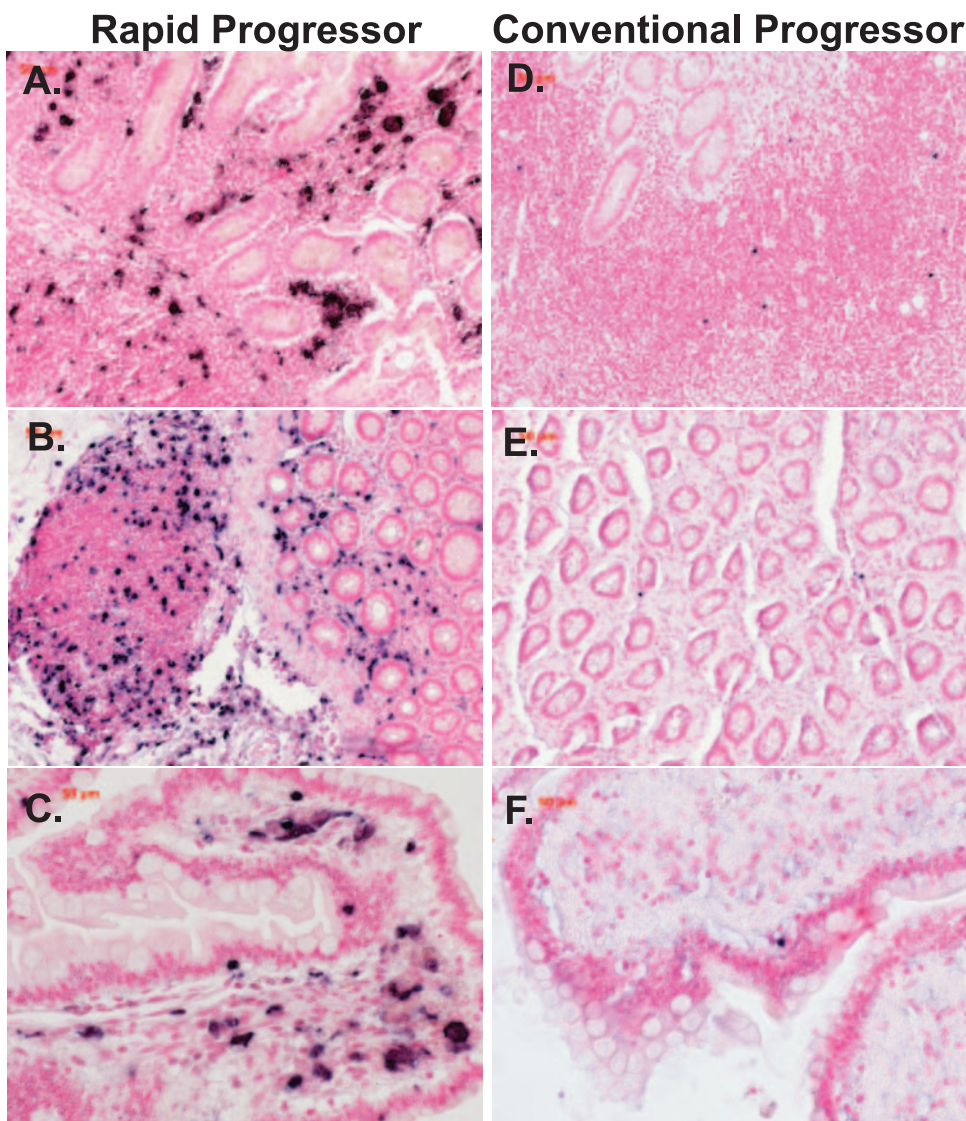
FIG. 5. Representative fields of view of ISH for SIV viral RNA in the ilea of RP (left) and CP (right) macaques. (A and B) Representative sections of the ilea of RP macaques H147 and H538 showing large numbers of SIV-expressing cells in the GALT, crypt regions, and lamina propria (magnification, ×10). Panel C shows a higher magnification of the ileum of macaque 18655 (magnification, ×40). (D, E, and F) Representative sections of the ilea of CP macaques H187 and H063 showing a scattering of SIV-expressing cells in the GALT (magnifications: D and E, ×10; F, ×40).

with only moderate blood CD4$^+$ T-cell depletion (Fig. 3B) (36). In contrast, CP macaques consistently showed severe depletion of total blood CD4$^+$ T cells at the time of euthanasia (Fig. 3A and B); terminal blood CD4$^+$ T cells were significantly lower in CP macaques than in RP macaques (Fig. 3B; Mann-Whitney U test, $P < 0.0001$).

Because of the retrospective nature of this study, CD4 subsets could not be evaluated in the majority of the animals. However, in a parallel study we examined CD4$^+$ T-cell subsets during disease progression in a cohort of 12 macaques (59). Memory and naive CD4$^+$ T-cell subsets of two representative RP (CK2F and CK2K) and CP (XGE and H679) macaques are detailed in Fig. 3C and D. These animals were typical for the RP and CP disease course and pathology, respectively (Table 1). All four animals experienced a dramatic decline in CD4$^+$

memory cells during the primary stage of infection (Fig. 3C), as previously observed by others (50, 66). However, partial replenishment of this T-cell subset only occurred in CP macaques, followed by a more precipitous decline terminally. The depletion of CD4$^+$ memory cells in RP macaques was rapid and progressive, reaching extremely low levels by the time of euthanasia. Naive CD4$^+$ T cells were preserved in RP macaques (Fig. 3D), as previously reported (59, 60, 66). In contrast, progressive loss of naive CD4$^+$ T cells was also observed in the CP macaques by the time of euthanasia (Fig. 3C, right). The total depletion of circulating CD4$^+$ T cells in the remainder of the cohort (Fig. 3A) is consistent with the depletion of both memory and naive subsets in these animals.

High virus expression in the lymph nodes and GI tracts of RP macaques. ISH to detect SIV expression in lymphoid

TABLE 2. Distribution and estimates of viral loads in tissues of SIV-infected rhesus macaques

Tissue[a]	RP[b]							CP[b]						
	147	168	538	567	445	426	18655	119	120	133	187	063	454	460
Lymphoid														
Thymus	2	4	3	1	3	2	2	1	0	0	0	1	1	1
ALN	2	2	4	4	4	2	3	1	1	1	2	1	1	1
ILN	3	3	4	4	3	2	4	1	1	1	2	1	1	1
TBLN	3	4	2	2	4	3	3	1	1	1	1	1	0	0
MLN	4	4	4	4	4	2	4	1	1	1	2	2	2	1
Spleen	3	2	4	4	4	1	4	1	1	1	2	1	1	1
Ileum	3	3	4	4	4	3	4	1	0	1	1	1	1	2
Colon	3	3	3	4	4	2	4	1	1	1	1	1	1	0
Nonlymphoid														
Lung	4	4	4	3	4	3	4	0	0	0	0	1	1	1
Liver	1	1	4	2	3	1	2	0	0	0	0	0	0	0
Kidney	3	2	2	3	3	2	3	0	0	0	0	1	0	0
Heart	2	3	2	2	2	2	2	0	0	0	0	0	0	0
Brain	2	3	4	4	3	3	4	1[c]	0	0	0	0	0	1
Spinal cord	2	3	2	1	ND	2	2	0	0	0	0	0	0	0
Eye	2	2	3	3	3	2	1	0	0	0	0	0	0	0
Uterus	NA	NA	4	3	NA	NA	NA	NA	NA	NA	NA	1	0	0
Ovary	NA	NA	4	ND	NA	NA	NA	NA	NA	NA	NA	0	0	0
Prostate	3	3	NA	NA	3	0	2	0	0	0	0	NA	NA	NA
Testis	3	3	NA	NA	2	1	3	0	0	0	1	NA	NA	NA

[a] ALN, axillary lymph node; ILN, inguinal lymph node; TBLN, tracheobronchial lymph node; MLN, mesenteric lymph node.
[b] 0, no SIV$^+$ cells observed in entire section; 1, rare SIV$^+$ cell per high-power field; 2, 1 to 5 SIV$^+$ cells per high-power field; 3, 5 to 10 SIV$^+$ cells per high-power field; 4, >10 SIV$^+$ cells per high-power field; ND, not determined; NA, not applicable.
[c] One focal area or a single positive cell was observed.

tissues and the GI tract revealed much higher expression levels in RP macaques at the time of euthanasia, as evident in representative lymph node (Fig. 4) and ileum (Fig. 5) sections. SIV-expressing cells in tissues of the RP macaques appeared to be primarily macrophages on the basis of their morphology, i.e., large, irregularly shaped cells containing abundant, foamy cytoplasm (Fig. 4C and 5C). In contrast, CP macaque tissues contained SIV-expressing cells that were small and round with a high nucleus-to-cytoplasm ratio, consistent with their identification as T cells (Fig. 4F and 5F). The difference in morphology between SIV$^+$ cells in RP and CP lymphoid tissues is clearly demonstrated by comparison of Fig. 4C and F.

The number of SIV-expressing cells in lymphoid tissues and the GI tract were assessed by scoring these tissues on a scale of 0 to 4. A score of 0 indicated that no SIV$^+$ cells were observed, whereas a score of 4 indicated >10 SIV$^+$ cells per field of view. As shown in Table 2, the number of virus-expressing cells was consistently higher in the lymphoid tissues and GI tracts of RP versus CP macaques. The majority of CP tissues scored at level 1 or lower (89%), whereas the majority of the scores for RP tissues were 3 or greater (73%). IPLab software was used to count the SIV-expressing cells in representative (40×) fields of the ileum and mesenteric lymph node sections of each of the RP and CP macaques. As shown in Fig. 6, the mean number of SIV-expressing cells in lymph nodes and the GALT and lamina propria of the ileum in samples collected at necropsy was significantly higher in RP macaques compared with CP macaques (Mann-Whitney U test).

Identification of target cells by confocal microscopy. Based on cell morphology in ISH-stained sections, the predominant cell type expressing SIV appeared to differ in RP and CP

macaques. Triple-label confocal microscopy with SIV-specific ISH (green) and immunohistochemistry for CD3$^+$ T cells (red) and HAM56$^+$ macrophages (white) was used to identify SIV-expressing cells in lymph nodes and the GI tract. Representative confocal fields from the mesenteric lymph nodes of RP and CP macaques are shown in Fig. 7A to D. The majority of SIV-expressing cells in the RP lymph nodes were identified as macrophages on the basis of coexpression of HAM56 (Fig. 7A and B). Rare SIV-expressing CD3$^+$ T cells were also identified (asterisks). In contrast, the majority of SIV-expressing cells in CP tissues were T cells on the basis of CD3 coexpression (Fig. 7C and D). Macrophages (HAM56) were also present but only rarely expressed SIV (not shown). To determine the proportion of SIV-expressing T cells and macrophages in tissues of RP and CP macaques, 10 representative fields of the lymph nodes or ileum of five RP and four CP macaques were photographed and the SIV$^+$ cells of each type were counted. As shown in Fig. 8A, similar numbers of SIV-infected T cells were observed in both RP and CP tissues. However, a large population of SIV-expressing macrophages was also observed in RP tissues such that SIV-infected macrophages greatly outnumbered T cells. The ratio of SIV$^+$ T cells to macrophages in CP macaques (Fig. 8B) was significantly higher than in RP macaque lymph nodes and GI tracts (0.97 versus 0.11; $P < 0.0001$), consistent with a difference in end stage target cell preference between the two disease courses.

Wider distribution of SIV expression in RP macaques by ISH. ISH for SIV viral RNA was used to examine the distribution of SIV-expressing cells in a variety of other, nonlymphoid, tissues such as lung, kidney, liver, reproductive tract, eye, and brain tissues. Representative fields of the latter
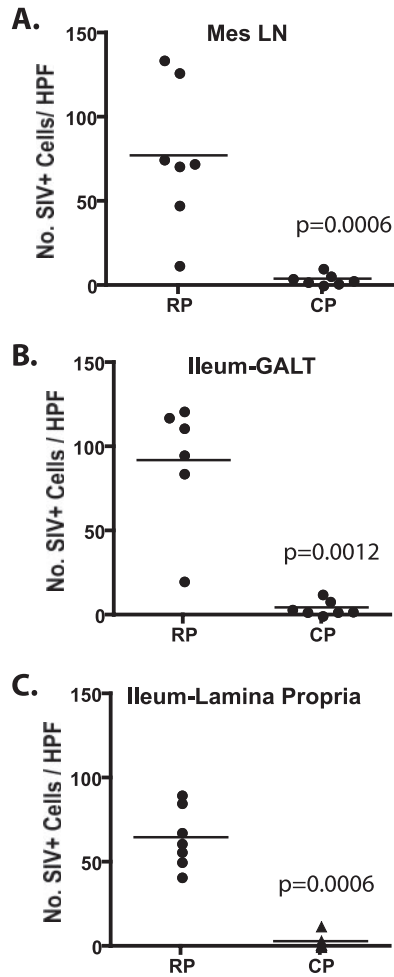
FIG. 6. Comparison of the numbers of SIV-expressing cells per high-power field (HPF) in the mesenteric lymph nodes and ilea of RP and CP macaques. Five random fields of view (magnification, ×40) of ISH-stained tissues from seven RP and seven CP macaques were photographed from each tissue, and the mean number of SIV$^+$ cells per high-power field for each tissue was calculated. Scatter plots of mean numbers of SIV$^+$ cells in the mesenteric lymph nodes (A), GALT (B), and lamina propria (C) of the ileum show that RP macaque tissues contained significantly more SIV$^+$ cells per high-power field compared to CP macaques (Mann-Whitney U test).

tissues are shown in Fig. 9. SIV-expressing giant cells were observed in the lung, choroid plexus, brain parenchyma, retina (Fig. 9A to D, respectively), glomeruli of the kidney (Fig. 9E), portal triads of the liver (Fig. 9F), and female and male urogenital tracts, respectively (Fig. 9G and H). This high level of expression of SIV in MNGC in nonlymphoid tissues was unique to the RP macaques. As detailed in the bottom half of Table 2, the distribution of virus expression in nonlymphoid tissues was much broader in the RP macaques than in CP macaques. SIV expression was generally only observed in the lymphoid tissues and GI tracts of CP macaques, whereas virus expression was observed in tissue macrophages residing in virtually every tissue of RP macaques that was examined, including privileged compartments such as the eye, brain, and testes.

DISCUSSION

This study demonstrates that RP macaques form a distinct group among SIVsmE660- and E543-3-inoculated macaques that is unique in terms of pathology and, by inference, pathogenesis. The end stage tissues we examined from RP macaques in this study exhibited primary SIV-induced pathological lesions in lymphoid tissues, as well many other, nonlymphoid, tissues. Despite evidence of immune suppression, OIs were rarely observed in RP macaques and thus their severe disease is presumably due to a direct effect of SIV replication in tissues, particularly in the lymphoid tissues, lungs, intestinal tract, and brain. SIVE was strongly associated with rapid progression, and there was a strong preference for SIV replication in macrophages. In contrast, the clinical disease in CP macaques could often be attributed to infections with opportunistic pathogens, a pathological picture reminiscent of HIV-induced AIDS in humans.

The clinical phenomenon of rapid disease progression in SIV-infected macaques is clearly observed with all pathogenic SIVsm and SIVmac strains (42). However, the pathology in RP macaques has not been comprehensively compared with CP macaques in other SIV models. Thus, it is not certain whether RP macaques inoculated with other SIV strains would segregate so clearly from slower progressors, as observed for SIVsmE543 and SIVsmE660 in the present study. The pathological features that we associated with rapid progression, such as MNGC formation (4), macrophage tropism (2, 17, 55), SIV enteropathy (30, 43, 78), and SIVE (3, 61, 77, 81), are not unique to one specific strain of SIV. For example, previous studies of SIVmac239 and SIVsm strains have demonstrated that SIVE is highly associated with lack of SIV-specific antibody responses and a rapid disease course (3, 61, 77). Additionally, immunologic features such as transient SIV-specific immune responses and early depletion of memory CD4$^+$ T cells are similar between SIVmac239 and SIVsmE543-3-infected RP macaques (59, 60, 66). Although OIs were rare in the RP macaques in the present study, they have been observed in other RP macaques infected with other strains of SIV (61, 66). Previous studies of three of these RP macaques (H445, H538, H567) demonstrated that they are profoundly immunosuppressed, as evident by their lack of SIV-specific immune responses and inability to mount recall and new antigen responses (36). Therefore, the lack of detectable OIs in the present study may be a matter of timing, i.e., SIVsm-infected RP macaques develop clinical disease as a result of the severity of primary SIV lesions in the intestine, lungs, and central nervous system before the manifestations of other OIs become pathologically evident. Certainly, the SIV-induced lesions in the intestine and lungs are sufficient to explain the clinical deterioration of these animals. Nevertheless, the severity of the primary SIV lesions appeared to be more pronounced in SIVsmE660- and SIVsmE543-inoculated RP macaques compared to reports of SIVmac239-inoculated RP macaques.

What is responsible for the difference in end stage pathology in RP macaques compared to CP macaques? We hypothesized that primary SIV lesions observed in RP macaques were the result of an extremely high viral load, resulting in nearly complete elimination of memory CD4$^+$ T cells and redirection of
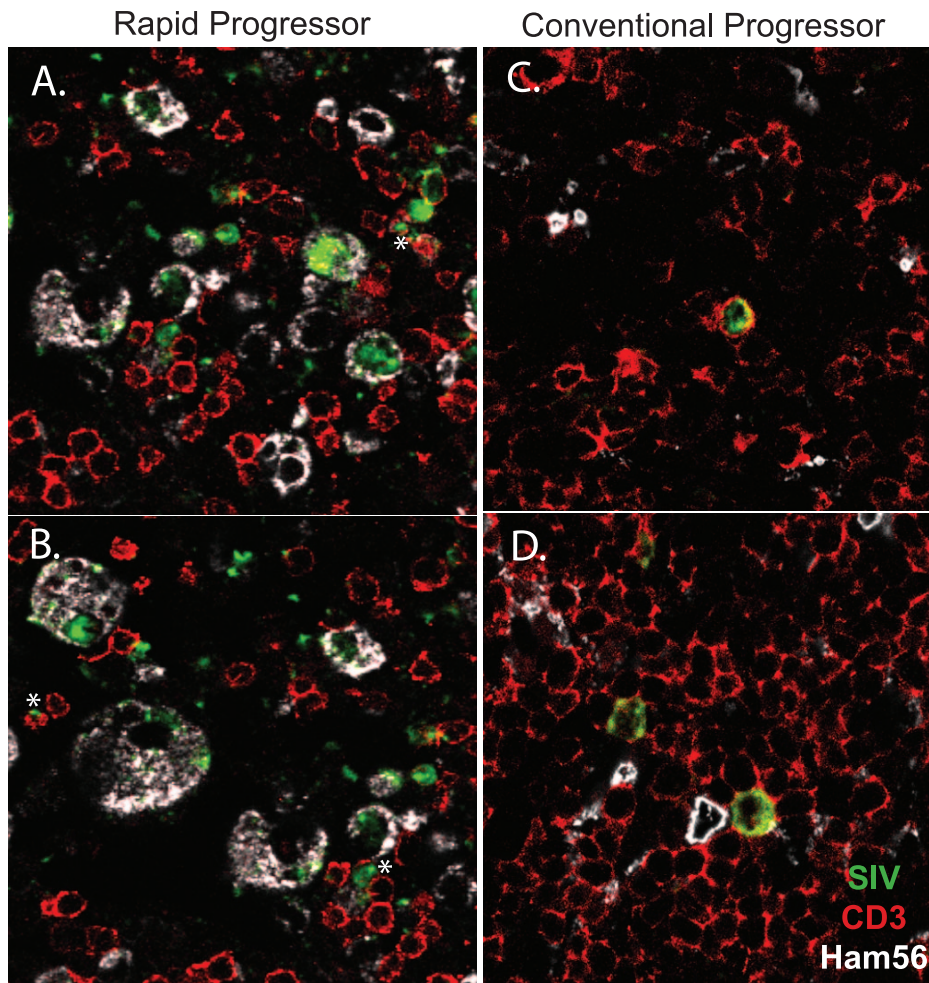
FIG. 7. Confocal microscopic analysis of mesenteric lymph nodes of representative RP and CP macaques. Triple-label confocal microscopy of lymph nodes from an RP macaque (A and B) and a CP macaque (C and D) to identify macrophages (HAM56, white), SIV RNA expression (ISH, green), and T cells (CD3, red). The majority of SIV-expressing cells in the tissues from the RP macaque coexpressed Ham56, a marker for macrophages (magnification, ×63). Rare CD3^{+} T cells coexpressing SIV are indicated by asterisks. In contrast (C and D), the majority of SIV-expressing cells in tissues of the CP macaques (H187 and H063) coexpressed CD3 (magnification, ×63).
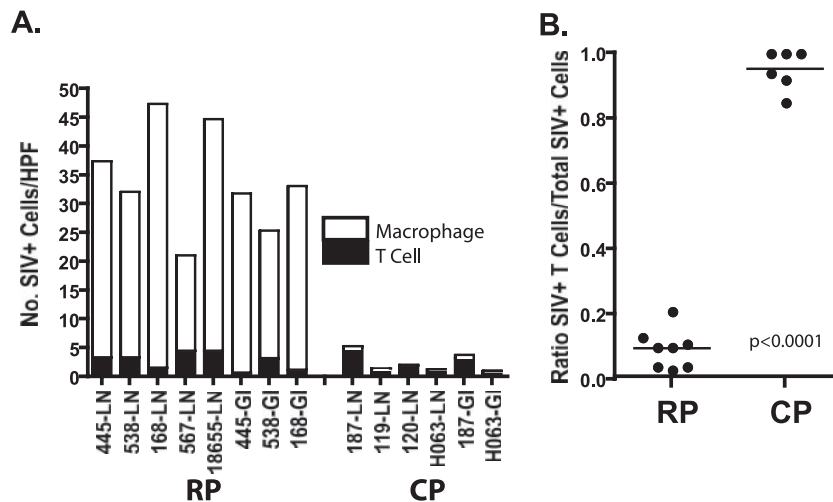
FIG. 8. Graphic representation of the proportions of SIV-expressing macrophages and T cells in the lymph nodes and ilea of RP and CP macaques. (A) The mean numbers of SIV^{+} cells per high-power field (HPF) of each type in various tissues of RP and CP macaques are shown by a bar graph where the filled bars represent T cells and the open bars represent macrophages. (B) Ratios of infected T cells to total infected cells in RP and CP tissues, demonstrating a significant difference between these two groups.
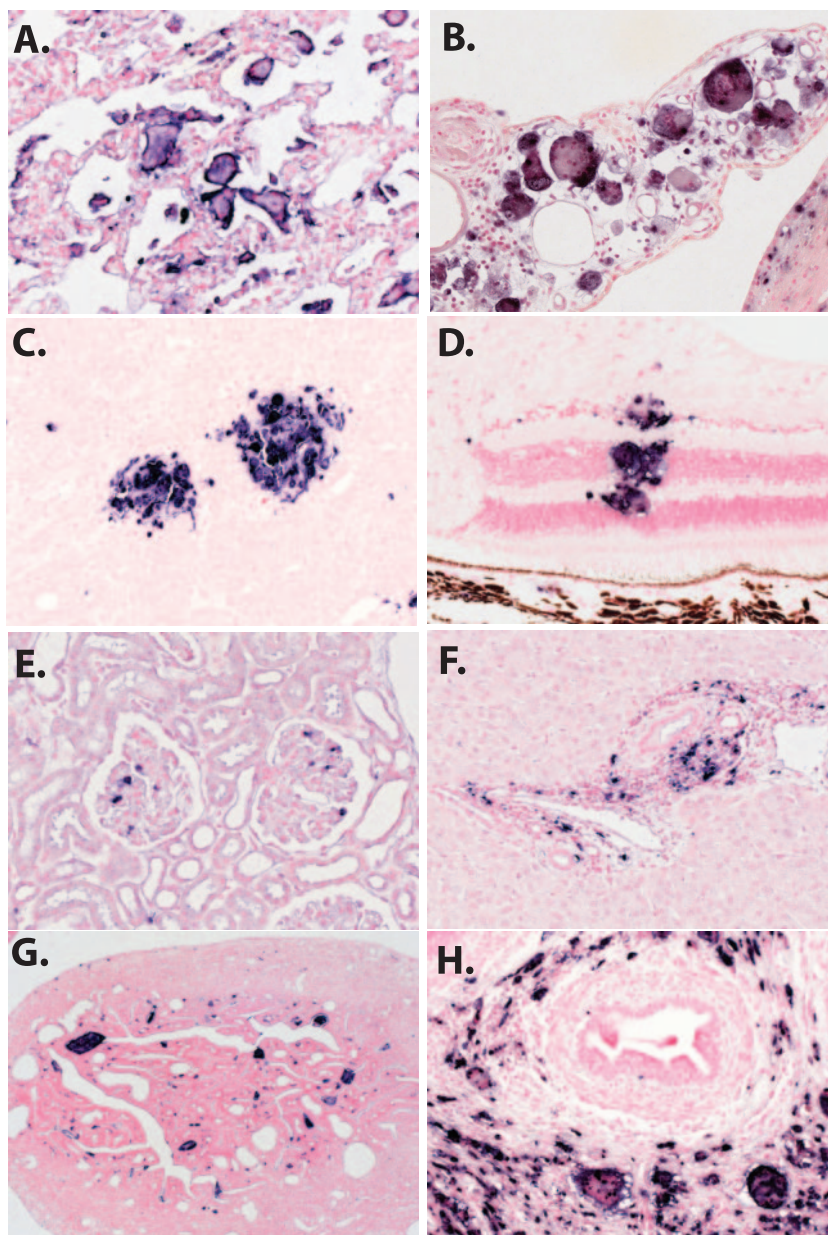
FIG. 9. ISH for SIV RNA in a wide range of tissues of RP macaques. (A) A section of lung tissue from RP macaque H168 shows abundant SIV-expressing giant cells (magnification, ×10). (B) SIV-expressing giant cells in the choroid plexus of macaque H567 (magnification, ×20). (C) ISH of the brain of RP macaque H567 showing perivascular infiltration of SIV-expressing macrophages and giant cells (magnification, ×10). (D) SIV-expressing macrophages in the retina of RP macaque H538 (magnification, ×20). (E) SIV-expressing cells within glomeruli of RP macaque H538. (F) SIV-expressing cells in periportal infiltrates in the liver of RP macaque H538. (G) SIV$^+$ giant cells in the interstitial areas of the fallopian tube of female macaque H538. (H) SIV-expressing cells adjacent to seminiferous tubules of male macaque H168.

the virus to infect tissue macrophages. Early destruction of mucosal CD4$^+$ T cells occurs in both RP and CP macaques (50, 59, 66, 75). However, compromised production and inadequate mucosal transport result in near total depletion of CD4$^+$ memory cells very early in the infection of SIV-infected RP macaques (59, 66). This loss is probably responsible for the failure of RP macaques to maintain SIV-specific immune responses, and as a consequence, RP macaques also do not develop the lymphadenopathy generally associated with hyperimmune activation in HIV and SIV infections. Consistent with

lack of immune activation, RP macaques show only transient increases in T-cell proliferation with declining levels of Ki-67-expressing CD4$^+$ T cells during disease progression (59). Loss of these cells as targets for the virus also presumably forces the virus to replicate in macrophages. This is similar to the scenario observed in X4-tropic SIV-HIV infections of macaques (39, 60), where total early loss of all CD4$^+$ T cells results in increased macrophage tropism (40, 41).

This forced adaptation to macrophages is probably also responsible for the specific evolution of SIV variants that we

have observed in previous studies of SIVsmE543-3-inoculated RP macaques (15, 46). Sequence analysis of viruses in three SIVsmE543-3-infected RP macaques (8) revealed a unique convergent pattern of substitutions in *env*, including the loss of a highly conserved potential glycosylation site in the V_1/V_2 region (N158D/S or S160N/G), substitutions in the cysteine loop that is analogous to HIV-1 V_3 (P337T/S/H/L and R348W), and substitutions in the highly conserved GDPE motif (G386R and D388N/V). These substitutions are associated with the development of CD4-independent use of CCR5 (15), which has previously been associated with an increased ability of viruses such as SIVmac316 to infect macrophages (56), as well as with increased sensitivity to neutralization (52). Both of these factors may drive the evolution of SIV in RP macaques and may be responsible for the difference in end stage pathology between RP and CP macaques.

The pathogenesis of CP macaques appears to be more similar to AIDS in humans than in RP macaques. CP macaques exhibit an early phase of memory CD4 T-cell loss at mucosal sites (7, 50); an asymptomatic phase characterized by persistent viremia and chronic immune activation (10, 13, 14, 70) with lymphadenopathy, lymphoid expansion, and fibrosis (69); eventual immunologic collapse; and development of OIs. Transient partial replenishment of memory $CD4^+$ T cells was observed in many CP macaques (59, 66). An increase in memory $CD4^+$ T-cell turnover, as assessed by Ki-67 expression, was observed in previous studies of CP macaques, and CD4 proliferation was sustained throughout the course of infection (59). As previously observed in other SIV studies (11, 71), CP macaques developed a lymphadenopathy also consistent with intense immune activation (8, 9). Similar to human AIDS, the onset of disease in CP macaques was associated with an overall decline in circulating $CD4^+$ T cells, including both memory and naive subsets (59). Despite the steady decline and the severe terminal $CD4^+$ T-cell depletion in CP macaques, a generalized switch or preference to infect macrophages was not observed. In addition to the early destruction of memory $CD4^+$ T cells, CP macaques also experience a slower loss of these cells during the chronic stages of infection that is accompanied by a significant loss of naive $CD4^+$ T cells (59).

It is not clear why naive $CD4^+$ T cells would be affected in CP macaques, since SIVsmE543-3 and SIVsmE660 use CCR5 for entry (15, 27). Since CCR5 is primarily expressed on memory $CD4^+$ T cells, depletion of this subset is an expected outcome. Evolution of CXCR4-using SIV variants such as seen in approximately 50% of late-stage human AIDS patients, is only rarely observed in SIV infection (44, 66). Although isolates from these animals were not examined for coreceptor use, a consistent switch to X4 tropism in each of these animals is unlikely. Indeed, loss of naive cells also occurs in HIV infection in the absence of the emergence of CXCR4-using variants. This makes the pattern of CD4 T-cell loss in CP macaques more similar to AIDS in humans. We speculate that the additional loss of naive $CD4^+$ T cells in CP macaques is not a direct result of virus-induced cell death. The decline in naive CD4 T cells by the terminal stages of disease is probably due to failure of the homeostatic and regenerative process from the continual, unrelenting loss of $CCR5^+$ memory $CD4^+$ T cells by virus killing and immune activation-induced cell death. Factors speculated to be involved include (i) exhaustion of the regen-

erative capacity of T-cell precursors to produce naive cells, (ii) bystander killing by immune activation-induced cell death, and (iii) limited repopulation and survival of T cells in lymphoid tissues damaged by collagen deposition (69).

The present study clearly demonstrated that rapid progression of SIV infection in macaques constitutes a pathological phenomenon that is distinct from classic AIDS. Nonetheless, the study of rapid progression to AIDS is important for a couple of reasons. First, RP macaques allow us to examine the direct effects of virus-induced cytopathology, uncomplicated by the secondary effects of immune activation-induced cell death seen in CP macaques. Second, it is important to understand the similarities and differences between SIV and HIV infections in using them as models for AIDS. Whereas the pathological and clinical descriptions of HIV-1 in humans are fairly uniform, SIV infection in macaques spans a wider spectrum of disease syndromes and pathological manifestations.

REFERENCES

1. **Allan, J. S., M. Short, M. E. Taylor, S. Su, V. M. Hirsch, P. R. Johnson, G. M. Shaw, and B. H. Hahn.** 1991. Species-specific diversity among simian immunodeficiency viruses from African green monkeys. J. Virol. **65:**2816–2828.
2. **Anderson, M. G., D. Hauer, D. P. Sharma, S. V. Joag, O. Narayan, M. C. Zink, and J. E. Clements.** 1993. Analysis of envelope changes acquired by SIV$_{mac}$239 during neuroadaption in rhesus macaques. Virology **195:**616–626.
3. **Baskin, G. B., C. M. Murphey, E. D. Roberts, P. J. Didier, and L. N. Martin.** 1992. Correlates of SIV encephalitis in rhesus monkeys. J. Med. Primatol. **21:**59–63.
4. **Baskin, G. B., M. Murphey-Corb, L. N. Martin, K. F. Soike, F. S. Hu, and D. Kuebler.** 1991. Lentivirus-induced pulmonary lesions in rhesus monkeys (Macaca mulatta) infected with simian immunodeficiency virus. Vet. Pathol. **28:**506–513.
5. **Baskin, G. B., M. Murphey-Corb, E. A. Watson, and L. N. Martin.** 1988. Necropsy findings in rhesus monkeys experimentally infected with cultured simian immunodeficiency virus (SIV)/delta. Vet. Pathol. **25:**456–467.
6. **Brenchley, J. M., D. A. Price, and D. C. Douek.** 2006. HIV disease: fallout from a mucosal catastrophe? Nat. Immunol. **7:**235–239.
7. **Brenchley, J. M., T. W. Schacker, L. E. Ruff, D. A. Price, J. H. Taylor, G. J. Beilman, P. L. Nguyen, A. Khoruts, M. Larson, A. T. Haase, and D. C. Douek.** 2004. CD4+ T cell depletion during all stages of HIV disease occurs predominantly in the gastrointestinal tract. J. Exp. Med. **200:**749–759.
8. **Chakrabarti, L., M. C. Cumont, L. Montagnier, and B. Hurtrel.** 1994. Variable course of primary simian immunodeficiency virus infection in lymph nodes: relation to disease progression. J. Virol. **68:**6634–6643.
9. **Chakrabarti, L., P. Isola, M. C. Cumont, M. M. Claessens, M. Hurtrel, L. Montagnier, and B. Hurtrel.** 1994. Early stages of simian immunodeficiency virus infection in lymph nodes. Evidence for high viral load and successive populations of target cells. Am. J. Pathol. **144:**1226–1237.
10. **Chakrabarti, L. A.** 2004. The paradox of simian immunodeficiency virus infection in sooty mangabeys: active viral replication without disease progression. Front. Biosci. **9:**521–539.
11. **Chalifoux, L. V., D. J. Ringler, N. W. King, P. K. Sehgal, R. C. Desrosiers, M. D. Daniel, and N. L. Letvin.** 1987. Lymphadenopathy in macaques experimentally infected with the simian immunodeficiency virus (SIV). Am. J. Pathol. **128:**104–110.
12. **Daniel, M. D., N. L. Letvin, N. W. King, M. Kannagi, P. K. Sehgal, R. D. Hunt, P. J. Kanki, M. Essex, and R. C. Desrosiers.** 1985. Isolation of T-cell tropic HTLV-III-like retrovirus from macaques. Science **228:**1201–1204.
13. **Deeks, S. G., C. M. Kitchen, L. Liu, H. Guo, R. Gascon, A. B. Narvaez, P. Hunt, J. N. Martin, J. O. Kahn, J. Levy, M. S. McGrath, and F. M. Hecht.** 2004. Immune activation set point during early HIV infection predicts subsequent CD4+ T-cell changes independent of viral load. Blood **104:**942–947.
14. **Deeks, S. G., and B. D. Walker.** 2004. The immune response to AIDS virus infection: good, bad, or both? J. Clin. Investig. **113:**808–810.
15. **Dehghani, H., B. A. Puffer, R. W. Doms, and V. M. Hirsch.** 2003. Unique pattern of convergent envelope evolution in simian immunodeficiency virus-infected rapid progressor macaques: association with CD4-independent usage of CCR5. J. Virol. **77:**6405–6418.

16. **Desrosiers, R. C.** 1990. The simian immunodeficiency viruses. Annu. Rev. Immunol. **8:**557–578.
17. **Desrosiers, R. C., A. Hansen-Moosa, K. Mori, D. P. Bouvier, N. W. King, M. D. Daniel, and D. J. Ringler.** 1991. Macrophage-tropic variants of SIV are associated with specific AIDS-related lesions but are not essential for the development of AIDS. Am. J. Pathol. **139:**29–35.
18. **Douek, D. C.** 2003. Disrupting T-cell homeostasis: how HIV-1 infection causes disease. AIDS Rev. **5:**172–177.
19. **Evans, D. T., L. A. Knapp, P. Jing, J. L. Mitchen, M. Dykhuizen, D. C. Montefiori, C. D. Pauza, and D. I. Watkins.** 1999. Rapid and slow progressors differ by a single MHC class I haplotype in a family of MHC-defined rhesus macaques infected with SIV. Immunol. Lett. **66:**53–59.
20. **Finkel, T. H., and N. K. Banda.** 1994. Indirect mechanisms of HIV pathogenesis: how does HIV kill T cells? Curr. Opin. Immunol. **6:**605–615.
21. **Finkel, T. H., G. Tudor-Williams, N. K. Banda, M. F. Cotton, T. Curiel, C. Monks, T. W. Baba, R. M. Ruprecht, and A. Kupfer.** 1995. Apoptosis occurs predominantly in bystander cells and not in productively infected cells of HIV- and SIV-infected lymph nodes. Nat. Med. **1:**129–134.
22. **Ganeshan, S., R. E. Dickover, B. T. Korber, Y. J. Bryson, and S. M. Wolinsky.** 1997. Human immunodeficiency virus type 1 genetic evolution in children with different rates of development of disease. J. Virol. **71:**663–677.
23. **Garland, F. C., C. F. Garland, E. D. Gorham, and S. K. Brodine.** 1996. Western blot banding patterns of HIV rapid progressors in the U.S. Navy Seropositive Cohort: implications for vaccine development. Ann. Epidemiol. **6:**341–347.
24. **Giorgi, J. V., L. E. Hultin, J. A. McKeating, T. D. Johnson, B. Owens, L. P. Jacobson, R. Shih, J. Lewis, D. J. Wiley, J. P. Phair, S. M. Wolinsky, and R. Detels.** 1999. Shorter survival in advanced human immunodeficiency virus type 1 infection is more closely associated with T lymphocyte activation than with plasma virus burden or virus chemokine coreceptor usage. J. Infect. Dis. **179:**859–870.
25. **Goldstein, S., C. R. Brown, H. Dehghani, J. D. Lifson, and V. M. Hirsch.** 2000. Intrinsic susceptibility of rhesus macaque peripheral CD4$^+$ T cells to simian immunodeficiency virus in vitro is predictive of in vivo viral replication. J. Virol. **74:**9388–9395.
26. **Gorry, P. R., G. Bristol, J. A. Zack, K. Ritola, R. Swanstrom, C. J. Birch, J. E. Bell, N. Bannert, K. Crawford, H. Wang, D. Schols, E. De Clercq, K. Kunstman, S. M. Wolinsky, and D. Gabuzda.** 2001. Macrophage tropism of human immunodeficiency virus type 1 isolates from brain and lymphoid tissues predicts neurotropism independent of coreceptor specificity. J. Virol. **75:**10073–10089.
27. **Grimm, T. A., B. E. Beer, V. M. Hirsch, and K. A. Clouse.** 2003. Simian immunodeficiency viruses from multiple lineages infect human macrophages: implications for cross-species transmission. J. Acquir. Immune Defic. Syndr. **32:**362–369.
28. **Grossman, Z., M. Meier-Schellersheim, A. E. Sousa, R. M. Victorino, and W. E. Paul.** 2002. CD4$^+$ T-cell depletion in HIV infection: are we closer to understanding the cause? Nat. Med. **8:**319–323.
29. **Hazenberg, M. D., D. Hamann, H. Schuitemaker, and F. Miedema.** 2000. T cell depletion in HIV-1 infection: how CD4$^+$ T cells go out of stock. Nat. Immunol. **1:**285–289.
30. **Heise, C., P. Vogel, C. J. Miller, C. H. Halsted, and S. Dandekar.** 1993. Simian immunodeficiency virus infection of the gastrointestinal tract of rhesus macaques. Functional, pathological, and morphological changes. Am. J. Pathol. **142:**1759–1771.
31. **Hirsch, V., D. Adger-Johnson, B. Campbell, S. Goldstein, C. R. Brown, W. R. Elkins, and D. C. Montefiori.** 1997. A molecularly cloned, pathogenic, neutralization-resistant simian immunodeficiency virus, SIVsmE543-3. J. Virol. **71:**1608–1620.
32. **Hirsch, V. M., G. Dapolito, P. R. Johnson, W. R. Elkins, W. T. London, R. J. Montali, S. Goldstein, and C. Brown.** 1995. Induction of AIDS by simian immunodeficiency virus from an African green monkey: species-specific variation in pathogenicity correlates with the extent of in vivo replication. J. Virol. **69:**955–967.
33. **Hirsch, V. M., T. R. Fuerst, G. Sutter, M. W. Carroll, L. C. Yang, S. Goldstein, M. J. Piatak, W. R. Elkins, W. D. Alvord, D. C. Montefiori, B. Moss, and J. D. Lifson.** 1996. Patterns of viral replication correlate with outcome in simian immunodeficiency virus (SIV)-infected macaques: effect of prior immunization with a trivalent SIV vaccine in modified vaccinia virus Ankara. J. Virol. **70:**3741–3752.
34. **Hirsch, V. M., and P. R. Johnson.** 1994. Pathogenic diversity of simian immunodeficiency viruses. Virus Res. **32:**183–203.
35. **Hirsch, V. M., R. A. Olmsted, M. Murphey-Corb, R. H. Purcell, and P. R. Johnson.** 1989. An African primate lentivirus (SIVsm) closely related to HIV-2. Nature **339:**389–392.
36. **Hirsch, V. M., S. Santra, S. Goldstein, R. Plishka, A. Buckler-White, A. Seth, I. Ourmanov, C. R. Brown, R. Engle, D. Montefiori, J. Glowczwskie, K. Kunstman, S. Wolinsky, and N. L. Letvin.** 2004. Immune failure in the absence of profound CD4$^+$ T-lymphocyte depletion in simian immunodeficiency virus-infected rapid progressor macaques. J. Virol. **78:**275–284.
37. **Hirsch, V. M., P. M. Zack, A. P. Vogel, and P. R. Johnson.** 1991. Simian immunodeficiency virus infection of macaques: end-stage disease is characterized by widespread distribution of proviral DNA in tissues. J. Infect. Dis. **163:**976–988.
38. **Holterman, L., H. Niphuis, P. J. ten Haaft, J. Goudsmit, G. Baskin, and J. L. Heeney.** 1999. Specific passage of simian immunodeficiency virus from end-stage disease results in accelerated progression to AIDS in rhesus macaques. J. Gen. Virol. **80**(Pt. 12):3089–3097.
39. **Igarashi, T., C. R. Brown, R. A. Byrum, Y. Nishimura, Y. Endo, R. J. Plishka, C. Buckler, A. Buckler-White, G. Miller, V. M. Hirsch, and M. A. Martin.** 2002. Rapid and irreversible CD4$^+$ T-cell depletion induced by the highly pathogenic simian/human immunodeficiency virus SHIV$_{DH12R}$ is systemic and synchronous. J. Virol. **76:**379–391.
40. **Igarashi, T., C. R. Brown, Y. Endo, A. Buckler-White, R. Plishka, N. Bischofberger, V. Hirsch, and M. A. Martin.** 2001. Macrophage are the principal reservoir and sustain high virus loads in rhesus macaques after the depletion of CD4$^+$ T cells by a highly pathogenic simian immunodeficiency virus/HIV type 1 chimera (SHIV): implications for HIV-1 infections of humans. Proc. Natl. Acad. Sci. USA **98:**658–663.
41. **Igarashi, T., H. Imamichi, C. R. Brown, V. M. Hirsch, and M. A. Martin.** 2003. The emergence and characterization of macrophage-tropic SIV/HIV chimeric viruses (SHIVs) present in CD4$^+$ T cell-depleted rhesus monkeys. J. Leukoc. Biol. **74:**772–780.
42. **Johnson, P. R., and V. M. Hirsch.** 1992. SIV infection of macaques as a model for AIDS pathogenesis. Int. Rev. Immunol. **8:**55–63.
43. **Kewenig, S., T. Schneider, K. Hohloch, K. Lampe-Dreyer, R. Ullrich, N. Stolte, C. Stahl-Hennig, F. J. Kaup, A. Stallmach, and M. Zeitz.** 1999. Rapid mucosal CD4$^+$ T-cell depletion and enteropathy in simian immunodeficiency virus-infected rhesus macaques. Gastroenterology **116:**1115–1123.
44. **Kodama, T., K. Mori, T. Kawahara, D. J. Ringler, and R. C. Desrosiers.** 1993. Analysis of simian immunodeficiency virus sequence variation in tissues of rhesus macaques with simian AIDS. J. Virol. **67:**6522–6534.
45. **Kunstman, K. J., B. Puffer, B. T. Korber, C. Kuiken, U. R. Smith, J. Kunstman, J. Stanton, M. Agy, R. Shibata, A. D. Yoder, S. Pillai, R. W. Doms, P. Marx, and S. M. Wolinsky.** 2003. Structure and function of CC-chemokine receptor 5 homologues derived from representative primate species and subspecies of the taxonomic suborders Prosimii and Anthropoidea. J. Virol. **77:**12310–12318.
46. **Kuwata, T., H. Dehghani, C. R. Brown, R. Plishka, A. Buckler-White, T. Igarashi, J. Mattapallil, M. Roederer, and V. M. Hirsch.** 2006. Infectious molecular clones from a simian immunodeficiency virus-infected rapid-progressor (RP) macaque: evidence of differential selection of RP-specific envelope mutations in vitro and in vivo. J. Virol. **80:**1463–1475.
47. **Letvin, N. L., and N. W. King.** 1990. Immunologic and pathologic manifestations of the infection of rhesus monkeys with simian immunodeficiency virus of macaques. J. Acquir. Immune Defic. Syndr. **3:**1023–1040.
48. **Li, Q., L. Duan, J. D. Estes, Z. M. Ma, T. Rourke, Y. Wang, C. Reilly, J. Carlis, C. J. Miller, and A. T. Haase.** 2005. Peak SIV replication in resting memory CD4$^+$ T cells depletes gut lamina propria CD4$^+$ T cells. Nature **434:**1148–1152.
49. **Lifson, J. D., M. A. Nowak, S. Goldstein, J. L. Rossio, A. Kinter, G. Vasquez, T. A. Wiltrout, C. Brown, D. Schneider, L. Wahl, A. L. Lloyd, J. Williams, W. R. Elkins, A. S. Fauci, and V. M. Hirsch.** 1997. The extent of early viral replication is a critical determinant of the natural history of simian immunodeficiency virus infection. J. Virol. **71:**9508–9514.
50. **Mattapallil, J. J., D. C. Douek, B. Hill, Y. Nishimura, M. Martin, and M. Roederer.** 2005. Massive infection and loss of memory CD4$^+$ T cells in multiple tissues during acute SIV infection. Nature **434:**1093–1097.
51. **McClure, H. M., D. C. Anderson, P. N. Fultz, A. A. Ansari, E. Lockwood, and A. Brodie.** 1989. Spectrum of disease in macaque monkeys chronically infected with SIV/SMM. Vet. Immunol. Immunopathol. **21:**13–24.
52. **Means, R. E., T. Greenough, and R. C. Desrosiers.** 1997. Neutralization sensitivity of cell culture-passaged simian immunodeficiency virus. J. Virol. **71:**7895–7902.
53. **Mellors, J. W., A. Munoz, J. V. Giorgi, J. B. Margolick, C. J. Tassoni, P. Gupta, L. A. Kingsley, J. A. Todd, A. J. Saah, R. Detels, J. P. Phair, and C. R. Rinaldo, Jr.** 1997. Plasma viral load and CD4$^+$ lymphocytes as prognostic markers of HIV-1 infection. Ann. Intern. Med. **126:**946–954.
54. **Michael, N. L., A. E. Brown, R. F. Voigt, S. S. Frankel, J. R. Mascola, K. S. Brothers, M. Louder, D. L. Birx, and S. A. Cassol.** 1997. Rapid disease progression without seroconversion following primary human immunodeficiency virus type 1 infection—evidence for highly susceptible human hosts. J. Infect. Dis. **175:**1352–1359.
55. **Mori, K., D. J. Ringler, T. Kodama, and R. C. Desrosiers.** 1992. Complex determinants of macrophage tropism in *env* of simian immunodeficiency virus. J. Virol. **66:**2067–2075.
56. **Mori, K., M. Rosenzweig, and R. C. Desrosiers.** 2000. Mechanisms for adaptation of simian immunodeficiency virus to replication in alveolar macrophages. J. Virol. **74:**10852–10859.
57. **Moss, A. R., and P. Bacchetti.** 1989. Natural history of HIV infection. AIDS **3:**55–61.
58. **Nishimura, Y., C. R. Brown, J. J. Mattapallil, T. Igarashi, A. Buckler-White, B. A. Lafont, V. M. Hirsch, M. Roederer, and M. A. Martin.** 2005. Resting naive CD4$^+$ T cells are massively infected and eliminated by X4-tropic

simian-human immunodeficiency viruses in macaques. Proc. Natl. Acad. Sci. USA 102:8000–8005.

59. Nishimura, Y., T. Igarashi, A. Buckler-White, C. Buckler, H. Imamichi, R. M. Goeken, W. R. Lee, B. A. Lafont, R. Byrum, H. C. Lane, V. M. Hirsch, and M. A. Martin. 2007. Loss of naive cells accompanies memory CD4+ T-cell depletion during long-term progression to AIDS in simian immunodeficiency virus-infected macaques. J. Virol. 81:893–902.

60. Nishimura, Y., T. Igarashi, O. K. Donau, A. Buckler-White, C. Buckler, B. A. Lafont, R. M. Goeken, S. Goldstein, V. M. Hirsch, and M. A. Martin. 2004. Highly pathogenic SHIVs and SIVs target different CD4+ T cell subsets in rhesus monkeys, explaining their divergent clinical courses. Proc. Natl. Acad. Sci. USA 101:12324–12329.

61. O'Neil, S. P., C. Suwyn, D. C. Anderson, G. Niedziela, J. Bradley, F. J. Novembre, J. G. Herndon, and H. M. McClure. 2004. Correlation of acute humoral response with brain virus burden and survival time in pig-tailed macaques infected with the neurovirulent simian immunodeficiency virus SIVsmmFGb. Am. J. Pathol. 164:1157–1172.

62. Orandle, M. S., K. C. Williams, A. G. MacLean, S. V. Westmoreland, and A. A. Lackner. 2001. Macaques with rapid disease progression and simian immunodeficiency virus encephalitis have a unique cytokine profile in peripheral lymphoid tissues. J. Virol. 75:4448–4452.

63. Ourmanov, I., C. R. Brown, B. Moss, M. Carroll, L. Wyatt, L. Pletneva, S. Goldstein, D. Venzon, and V. M. Hirsch. 2000. Comparative efficacy of recombinant modified vaccinia virus Ankara expressing simian immunodeficiency virus (SIV) Gag-Pol and/or Env in macaques challenged with pathogenic SIV. J. Virol. 74:2740–2751.

64. Piatak, M., Jr., K. C. Luk, B. Williams, and J. D. Lifson. 1993. Quantitative competitive polymerase chain reaction for accurate quantitation of HIV DNA and RNA species. BioTechniques 14:70–81.

65. Piatak, M., Jr., M. S. Saag, L. C. Yang, S. J. Clark, J. C. Kappes, K. C. Luk, B. H. Hahn, G. M. Shaw, and J. D. Lifson. 1993. High levels of HIV-1 in plasma during all stages of infection determined by competitive PCR. Science 259:1749–1754.

66. Picker, L. J., S. I. Hagen, R. Lum, E. F. Reed-Inderbitzin, L. M. Daly, A. W. Sylwester, J. M. Walker, D. C. Siess, M. Piatak, Jr., C. Wang, D. B. Allison, V. C. Maino, J. D. Lifson, T. Kodama, and M. K. Axthelm. 2004. Insufficient production and tissue delivery of CD4+ memory T cells in rapidly progressive simian immunodeficiency virus infection. J. Exp. Med. 200:1299–1314.

67. Pitcher, C. J., S. I. Hagen, J. M. Walker, R. Lum, B. L. Mitchell, V. C. Maino, M. K. Axthelm, and L. J. Picker. 2002. Development and homeostasis of T cell memory in rhesus macaque. J. Immunol. 168:29–43.

68. Rutherford, G. W., A. R. Lifson, N. A. Hessol, W. W. Darrow, P. M. O'Malley, S. P. Buchbinder, J. L. Barnhart, T. W. Bodecker, L. Cannon, L. S. Doll, et al. 1990. Course of HIV-I infection in a cohort of homosexual and bisexual men: an 11 year follow up study. BMJ 301:1183–1188.

69. Schacker, T. W., P. L. Nguyen, G. J. Beilman, S. Wolinsky, M. Larson, C. Reilly, and A. T. Haase. 2002. Collagen deposition in HIV-1 infected lymphatic tissues and T cell homeostasis. J. Clin. Investig. 110:1133–1139.

70. Silvestri, G., A. Fedanov, S. Germon, N. Kozyr, W. J. Kaiser, D. A. Garber, H. McClure, M. B. Feinberg, and S. I. Staprans. 2005. Divergent host responses during primary simian immunodeficiency virus SIVsm infection of natural sooty mangabey and nonnatural rhesus macaque hosts. J. Virol. 79:4043–4054.

71. Simon, M. A., S. J. Brodie, V. G. Sasseville, L. V. Chalifoux, R. C. Desrosiers, and D. J. Ringler. 1994. Immunopathogenesis of SIVmac. Virus Res. 32:227–251.

72. Sopper, S., U. Sauer, J. G. Muller, C. Stahl-Hennig, and V. ter Meulen. 2000. Early activation and proliferation of T cells in simian immunodeficiency virus-infected rhesus monkeys. AIDS Res. Hum. Retrovir. 16:689–697.

73. Staprans, S. I., P. J. Dailey, A. Rosenthal, C. Horton, R. M. Grant, N. Lerche, and M. B. Feinberg. 1999. Simian immunodeficiency virus disease course is predicted by the extent of virus replication during primary infection. J. Virol. 73:4829–4839.

74. Suryanarayana, K., T. A. Wiltrout, G. M. Vasquez, V. M. Hirsch, and J. D. Lifson. 1998. Plasma SIV RNA viral load determination by real-time quantification of product generation in reverse transcriptase-polymerase chain reaction. AIDS Res. Hum. Retrovir. 14:183–189.

75. Veazey, R. S., M. DeMaria, L. V. Chalifoux, D. E. Shvetz, D. R. Pauley, H. L. Knight, M. Rosenzweig, R. P. Johnson, R. C. Desrosiers, and A. A. Lackner. 1998. Gastrointestinal tract as a major site of CD4+ T cell depletion and viral replication in SIV infection. Science 280:427–431.

76. Watson, A., J. Ranchalis, B. Travis, J. McClure, W. Sutton, P. R. Johnson, S. L. Hu, and N. L. Haigwood. 1997. Plasma viremia in macaques infected with simian immunodeficiency virus: plasma viral load early in infection predicts survival. J. Virol. 71:284–290.

77. Westmoreland, S. V., E. Halpern, and A. A. Lackner. 1998. Simian immunodeficiency virus encephalitis in rhesus macaques is associated with rapid disease progression. J. Neurovirol. 4:260–268.

78. Zeitz, M., R. Ullrich, T. Schneider, S. Kewenig, K. Hohloch, and E. O. Riecken. 1998. HIV/SIV enteropathy. Ann. N. Y. Acad. Sci. 859:139–148.

79. Zhang, J. Y., L. N. Martin, E. A. Watson, R. C. Montelaro, M. West, L. Epstein, and M. Murphey-Corb. 1988. Simian immunodeficiency virus/delta-induced immunodeficiency disease in rhesus monkeys: relation of antibody response and antigenemia. J. Infect. Dis. 158:1277–1286.

80. Zhang, L., T. He, Y. Huang, Z. Chen, Y. Guo, S. Wu, K. J. Kunstman, R. C. Brown, J. P. Phair, A. U. Neumann, D. D. Ho, and S. M. Wolinsky. 1998. Chemokine coreceptor usage by diverse primary isolates of human immunodeficiency virus type 1. J. Virol. 72:9307–9312.

81. Zink, M. C., A. M. Amedee, J. L. Mankowski, L. Craig, P. Didier, D. L. Carter, A. Munoz, M. Murphey-Corb, and J. E. Clements. 1997. Pathogenesis of SIV encephalitis. Selection and replication of neurovirulent SIV. Am. J. Pathol. 151:793–803.

82. Zink, M. C., K. Suryanarayana, J. L. Mankowski, A. Shen, M. Piatak, Jr., J. P. Spelman, D. L. Carter, R. J. Adams, J. D. Lifson, and J. E. Clements. 1999. High viral load in the cerebrospinal fluid and brain correlates with severity of simian immunodeficiency virus encephalitis. J. Virol. 73:10480–10488.